Teo, I., Sedgwick, B., Kilpatrick, M. W., McCarthy, T. V., & Lindahl, T. (1986) *Cell 45*, 315–324.
Vallee, B. L., & Auld, D. S. (1990a) *Proc. Natl. Acad. Sci. U.S.A. 87*, 220–224.
Vallee, B. L., & Auld, D. S. (1990b) *Biochemistry 29*, 5647–5659.
Yoshikai, T., Nakabeppu, Y., & Sekiguchi, M. (1988) *J. Biol. Chem. 263*, 19174–19180.

Articles

Purification, Characterization, and Fibrinogen Cleavage Sites of Three Fibrinolytic Enzymes from the Venom of *Crotalus basiliscus basiliscus*†

Anastassios D. Retzios and Francis S. Markland, Jr.*

Department of Biochemistry, School of Medicine, University of Southern California, 1303 North Mission Road, CRL 106, Los Angeles, California 90033

Received July 23, 1991; Revised Manuscript Received February 19, 1992

ABSTRACT: Three distinct fibrinolytic enzymes have been purified from the venom of *Crotalus basiliscus basiliscus* (the Mexican west coast rattlesnake). The high-performance liquid chromatography-based purification comprised the following steps: (a) hydrophobic interaction chromatography; (b) hydroxylapatite chromatography; (c) anion-exchange chromatography. Following hydrophobic interaction chromtography two fibrinolytic activity peaks were detected, Cbfib1 and Cbfib2. Cbfib2 was rendered homogeneous following hydroxylapatite chromatography. Upon hydroxylapatite chromatography Cbfib1 was shown to consist of two components, Cbfib1.1 and Cbfib1.2. Both Cbfib1.1 and Cbfib1.2 were purified to homogeneity using anion-exchange chromatography. SDS–polyacrylamide gel electrophoresis revealed that Cbfib1.1 and Cbfib1.2 had similar molecular weights (approximately 23 500), whereas Cbfib2 displayed a molecular weight of approximately 22 500. The enzymes do not appear to be glycosylated. Tryptic digests of all three enzymes, analyzed by high-performance reverse-phase chromatography, suggest that Cbfib1.1 and Cbfib1.2 are closely related and different from Cbfib2. The latter displayed more similarity with Cbfib1.2 than with Cbfib1.1. Specific fibrinolytic activity for all three enzymes was very similar, but general proteolytic activity varied substantially with Cbfib2 showing a 12-fold higher specific proteolytic activity when compared to Cbfib1.1 and Cbfib1.2. None of these enzymes exhibited hemorrhagic activity when injected (up to 100 μg) subcutaneously into mice. Cbfib1.1 and Cbfib1.2 action against fibrinogen was directed equally against both the Aα- and Bβ-chains. Against fibrin the rate of degradation of the α-chain was considerably higher than that of the β-chain. Cbfib2 showed mainly α-fibrin(ogen)ase activity with limited activity on the β-chain. Several fibrinogen cleavage sites on the Aα-chain have been identified: Cbfib1.1 and Cbfib1.2 cleave at Lys^{413}–Leu^{414}, Ser^{505}–Thr^{506}, and Tyr^{560}–Ser^{561}. Cbfib2 cleaves mainly at Gly^{254}–Ser^{255} and Pro^{516}–Met^{517}.

A number of enzymes that influence blood coagulation have been isolated from various snake venoms. These enzymes can either promote or inhibit coagulation (Markland & Damus, 1971; Ouyang & Teng, 1972; Holeman & Weiss, 1976; Teng & Seegers, 1981). Fibrinolytic activities have received special attention because of their possible therapeutic role for dissolution of blood clots (Didisheim & Lewis, 1956) and because they may serve as templates for the development of de novo agents.

Fibrinolytic enzymes have been identified in the venom of several *Agkistrodon* species such as *contortrix*, *acutus*, and *piscivorus* [Kornalik (1966), Ouyang and Teng (1972), and Moran and Geren (1981), respectively]. A fibrinolytic enzyme from the venom of *Agkistrodon contortrix contortrix* (southern copperhead snake) has been purified and characterized by this laboratory (Markland et al., 1988; Guan et al., 1991). This enzyme (fibrolase or Accfib[1]) is a zinc metalloproteinase (1 mol of zinc/mol of enzyme) with a molecular weight close to 23 800. It readily cleaves the α- and Aα-chains of fibrin and fibrinogen, respectively, between Lys^{413}–Leu^{414}, without activating or degrading plasminogen or protein C (Retzios & Markland, 1988). A similar enzyme, Apcfib, has been purified from the venom of *Agkstrodon piscivorus conanti* (Florida cottonmouth) (Retzios & Markland, 1990). In vivo Accfib has been shown to dissolve aged clots in the renal arteries and iliac veins of rabbits (Markland et al., 1989). It may, therefore, have significant clinical potential. A nonhemorrhagic fibrinolytic enzyme, called atroxase, has also been

†This study has been supported in part by NIH Grant HL 31389 from the USPHS and by Cortech, Inc., Denver, CO.

[1] Abbreviations: Accfib, fibrinolytic enzyme from *Agkistrodon contortrix contortrix* (southern copperhead) venom, also known as fibrolase; Apcfib, fibrinolytic enzyme from *Agkistrodon piscivorus conanti* (Florida cottonmouth) venom; Cbfib1.1, Cbfib1.2, and Cbfib2, fibrinolytic enzymes from *Crotalus basiliscus basiliscus* (Mexican west coast rattlesnake) venom; SDS–PAGE, sodium dodecyl sulfate–polyacrylamide gel electrophoresis; DTT, dithiothreitol; TPCK, *N*-tosyl-L-phenylalanine chloromethyl ketone; PIU, plasmin international units of activity; SBTI, soybean trypsin inhibitor; PMSF, phenylmethanesulfonyl fluoride; HPLC, high-performance liquid chromatography; Zincov, 2-(*N*-hydroxycarbamoyl)-4-methylpentanoyl-L-alanylglycine amide.

0006-2960/92/0431-4547$03.00/0

purified from the venom of *Crotalus atrox* (Willis & Tu, 1988). This enzyme is a zinc metalloprotease with a molecular weight similar to that of Accfib; its in vivo activity has been studied in rats (Willis et al., 1989).

In the present study we report the isolation and characterization of three distinct zinc-dependent fibrinolytic metalloproteinases from the venom of *Crotalus basiliscus basiliscus* (Mexican west coast rattlesnake). Their properties and mode of action against fibrin and fibrinogen have been examined and compared to those of Accfib and Apcfib. These studies along with those previously reported (Retzios & Markland, 1988) represent the first reports of peptide bond specificity of snake venom fibrinolytic enzymes on the presumably natural substrates, fibrin or fibrinogen. The Cbfib enzymes, apart from their significance as potential clinical agents, display bond cleavage specificities in variance with metalloproteinases studied to date.

Materials and Methods

Materials. HPLC-grade solvents and chemicals were purchased from VWR Scientific, Cerritos, CA; HPLC-grade trifluoroacetic acid was purchased from Pierce, Redford, TN. Venoms were obtained from Biotoxins, Inc., St. Cloud, FL. Plasminogen-free human fibrinogen (Kabi Diagnostica, grade L) was obtained from Helena Laboratories, Beaumont, TX. Standard human plasmin (Second International Reference Preparation) was obtained from the National Institute for Biological Standards and Control, London, U.K. Accfib was prepared according to the method described by Retzios and Markland (1990). *N*-Tosyl-L-phenylalanine chloromethyl ketone (TPCK) treated trypsin was obtained from Worthington Biochemical Corp., Freehold, NJ. Reagents for immunoblotting were purchased from Sigma Chemical Co., St. Louis, MO. Zincov was purchased from Calbiochem, La Jolla, CA. All other reagents were of analytical grade.

Instruments. Purification of the fibrinolytic enzymes was performed on a Perkin-Elmer 410 Bio HPLC system equipped with the LC-95 variable-wavelength detector and LC-100 integrator. Reverse-phase chromatography for the evaluation of purity of preparations, tryptic digest analysis, and isolation of fibrinogen fragments was performed on a Spectra-Physics 8800 HPLC system equipped with a Spectra-Physics 8450 variable-wavelength detector. Both systems were connected to the Spectra-Physics WINner data acquisition module.

Columns. For hydrophobic interaction chromatography, the polypropylaspartamide column (21 mm × 250 mm) from PolyLC, Columbus, OH, was employed. Hydroxylapatite chromatography was performed on a SynChropak HAP-5 hydroxylapatite column (21.2 mm × 100 mm) from SynChrom, Inc., Lafayette, IN. Anion-exchange chromatography was performed on a semipreparative SynChropak AX-300 column (10 mm × 250 mm) from SynChrom, Inc. Reverse-phase chromatography was performed on C_4 (214TP54) or C_{18} (218TP54) columns (4.1 mm × 250 mm) from Vydac, Hesperia, CA.

Purification Methodology. Purification of fibrinolytic enzymes from the venom of *Crotalus basiliscus* was accomplished by the use of a three-step HPLC-based chromatography procedure as described below.

(A) Hydrophobic Interaction Chromatography. The preparative polypropylaspartamide column was employed for the first step. The column was equilibrated with buffer A (0.1 M sodium phosphate buffer, pH 6.8, containing 1.0 M ammonium sulfate and 0.05% NaN_3). Venom, 1 g dissolved in 12 mL of buffer A, was centrifuged, filtered, and added to the column. Elution was then carried out by a linear increase in the concentration of buffer B (0.1 M sodium phosphate buffer, pH 6.8, containing 0.05% NaN_3). The flow rate was kept constant at 3 mL/min. The following elution protocol was used: (a) after injection of venom the column was washed with buffer A for 25 min; (b) a linear gradient to 100% buffer B was established over 90 min; (c) elution was completed by maintaining 100% buffer B isocratically for 60 min.

(B) Hydroxylapatite Chromatography. Fibrinolytic activity pools resulting from hydrophobic interaction HPLC were concentrated by 80% ammonium sulfate precipitation and dialyzed against 0.01 M sodium phosphate buffer, pH 6.8. The SynChropak hydroxylapatite HPLC column was equilibrated with 0.01 M sodium phosphate buffer, pH 6.8, containing 0.05% NaN_3 and 0.3 mM $CaCl_2$ (buffer A). Elution was performed with a linear gradient of buffer B (0.35 M sodium phosphate buffer, pH 6.8, containing 0.05% NaN_3 and 0.3 mM $CaCl_2$). The flow rate was kept constant at 2 mL/min. The following elution protocol was employed: (a) after addition of the sample the column was washed with buffer A for 15 min; (b) a linear gradient to 60% buffer B was run over 110 min; (c) this was followed with a linear gradient to 100% buffer B over 35 min; (d) the run was completed with isocratic elution at 100% buffer B for 30 min.

(C) Anion-Exchange Chromatography. Pooled fibrinolytic fractions after hydroxylapatite HPLC were concentrated by ammonium sulfate precipitation and dialyzed against 0.01 M sodium phosphate buffer, pH 6.8. The dialyzates were subsequently injected onto the AX-300 column equilibrated with 0.01 M sodium phosphate buffer, pH 6.8, containing 0.05% NaN_3 (buffer A). Elution was achieved by a linear gradient with buffer B (0.01 M sodium phosphate buffer, pH 6.8, containing 1.0 M NaCl and 0.05% NaN_3). The flow rate was 1 mL/min. The following elution protocol was employed: (a) after the addition of the sample the column was washed with buffer A for 20 min; (b) a linear gradient to 100% buffer B was established over 120 min; (c) this was followed by isocratic elution at 100% buffer B for 25 min.

Tryptic Digest Mapping. Prior to tryptic digestion the enzymes were reduced and carboxymethylated using the following procedure. The fibrinolytic enzymes (2.5 mg) were dialyzed against water, freeze-dried, and dissolved in 2 mL of 0.2 M Tris buffer, pH 8.2, containing 8 M urea. Dithiothreitol (1 mg) was added to each solution (3.2 mM DDT final concentration), and the mixtures were incubated at 37 °C for 1 h. Iodoacetamide (2 mg) was then added to each tube (5.4 mM iodoacetamide final concentration); the tubes were sealed under oxygen-free nitrogen and incubated in the dark in 1 h at room temperature. Iodoacetamide treatment was repeated to ensure completeness of the reaction. Following carboxymethylation the enzymes were dialyzed against water and freeze-dried. The carboxymethylated enzymes were dissolved in 1 mL of 0.2 M Tris buffer, pH 8.7, containing 2 M urea. TPCK-treated trypsin was added at a ratio of 1/40 (w/w, trypsin/fibrinolytic enzyme). Digestion was allowed to proceed at room temperature, with continuous stirring, for 24 h. Following digestion, the tryptic peptides were separated by reverse-phase chromatography. Each digest (100 μL) was added to a Vydac C_{18} column, and digestion products were eluted using the following protocol: (a) 5 min isocratically at 90% solvent A (0.1% TFA in water) and 10% solvent B (0.1% TFA in 80% acetonitrile); (b) 80-min linear gradient to 65% solvent B.

SDS–Polyacrylamide Gel Electrophoresis. SDS–PAGE was carried out according to the method of Laemmli (1970). Standards used for molecular weight determination were ob-

tained from Bio-Rad (phosphorylase *b*, 97.4 kDa; bovine serum albumin, 66.2 kDa; ovalbumin, 45 kDa; carbonic anhydrase, 31 kDa; soybean trypsin inhibitor, 21.5 kDa; and lysozyme, 14.4 kDa) or from Sigma (bovine serum albumin, 66 kDa; ovalbumin, 45 kDa; glyceraldehyde-3-phosphate dehydrogenase, 36 kDa; carbonic anhydrase, 29 kDa; trypsinogen, 24 kDa; soybean trypsin inhibitor, 20.4/19.7 kDa; α-lactalbumin, 14 kDa). Staining was with Coomassie brilliant blue R250 (Sigma) or Coomassie followed by silver staining (Bio-Rad) using the method of Merrill et al. (1983).

Isoelectric Focusing. The Bio-Rad mini IEF gel apparatus, model 111, attached to an Ortec 4100 constant power supply, and Bio-Rad ampholyte solutions were used for the determination of the isoelectric points (p*I*) of the purified proteins. IEF standard protein of known p*I* was obtained from Bio-Rad. Staining was with Coomassie blue R250 and crocein scarlet.

Carbohydrate Analysis. Carbohydrate was determined by the periodic acid–silver staining procedure after SDS–PAGE as described by Dubray and Bezard (1982). In our hands, the detectable amount of carbohydrate by this procedure is 0.28 μg using horseradish peroxidase (which contains 18% carbohydrate) as a positive control.

Amino Acid Analysis. Amino acid compositions of the reduced–carboxymethylated proteins were obtained by the method of Bidlingmeyer et al. (1984). Analyses were performed on the protein samples hydrolyzed in the vapor of constant boiling HCl containing 1% (v/v) phenol for 24 h, in vacuo, at 110 °C. Phenylthiocarbamoyl-amino acids were separated by reverse-phase HPLC using a Nova-Pak C_{18} reverse-phase column.

Proteolytic Activity. This was assessed by azocasein hydrolysis. Azocasein was synthesized from α-casein and diazotized sulfanilamide (Charney & Tomarelli, 1947). The resulting azocasein solution in 1% sodium bicarbonate had a concentration of 42 mg/mL. To measure proteolytic activity, 0.75 mL of the azocasein solution was added to a 1.5-mL microcentrifuge tube. The test solution containing fibrinolytic enzyme (50 μL) was added, and the tube was incubated at 37 °C for 30 min. The reaction was stopped by the addition of 0.75 mL of 1.16 M perchloric acid, and the resulting precipitate was removed by centrifugation. Hydrolysis of azocasein was measured as increased absorbance at 390 nm of the supernatant, using as reference azocasein treated in an identical manner but without enzyme. To accurately estimate specific activity (absorbance units 390 nm/mg of enzyme), varying quantities of the enzymes were added in order to construct a response curve. The linear part of the curve was used for the estimation of specific proteolytic activity.

Fibrinolytic Activity. Fibrinolytic activity was measured with the fibrin-plate-clearance assay (Bajwa et al., 1980). To measure areas of lysis accurately, at the end of the incubation period the plates are flooded with 10% TCA solution. The diameters of the lysis areas are then measured against a dark background. As with the proteolytic assay, several enzyme dilutions were tested in order to construct a response curve. A standard response curve is constructed using a solution of reference plasmin (0.5 plamin international units (PIU)/mL) in 0.1 M Tris, pH 7.8, containing 0.05 M NaCl, and fibrinolytic activity is expressed in PIU.

Hemorrhagic Activity. Hemorrhagic activity of the purified fibrinolytic enzymes was evaluated by a modification of the skin test procedure of Kondo et al. (1960). In this method, purified enzyme (50–100 μg) is injected subdermally under the clean shaven backs of white mice (approximately 20 g in weight). After 18 h the animals are sacrificed, the skin is removed, and the area of hemorrhage on the underside of the skin is measured.

Inhibition Studies. To determine the effect of EDTA on enzyme activity, 50 μL of 97.5 μM Cbfib1.1 or 94.2 μM Cbfib2 was added to separate reaction tubes. Buffer (0.1 M Tris, 0.05 M NaCl, pH 8.4) containing EDTA was added to a final volume of 0.5 mL such that the molar ratio of EDTA to enzyme was approximately 200, 400, 1000, and 5000. The resulting solutions were stirred continuously at room temperature for 30 min, and aliquots were removed for azocasein assay at 5-min intervals.

The effect of Zincov [2-(*N*-hydroxycarbamoyl)-4-methylpentanoyl-L-alanylglycine amide] on the enzymes was analyzed using a modification of the azocasein assay. A stock solution of 16.5 mM Zincov in azocasein solution (50 mg/mL) was prepared, and several Zincov concentrations were obtained by diluting the stock solution into the azocasein solution. Azocasein solution (0.75 mL) containing 16.5, 8.25, 4.12, 2.06, 1.03, or 0 mM Zincov was added to microcentrifuge tubes and warmed to 37 °C. The enzyme (50 μL of 45.9 μM Cbfib1.1 or 41 μM Cbfib2) was then added. The enzymes had been preincubated with Zincov, at the concentrations noted above, at room temperature for 15 min. After addition of enzyme the azocasein solution was incubated at 37 °C for 30 min, and the reaction was stopped by the addition of 0.75 mL of 1.16 mM perchloric acid. Activity was estimated by measuring absorbance at 390 nm (see Proteolytic Activity).

To study the effect of PMSF, 10 μL (150 mM in ethanol) was added to 440 μL of 0.1 M Tris buffer, pH 8.4, containing 0.05 M NaCl, and Cbfib1.1 (50 μL of 45.9 μM solution) was quickly added. The resulting solution was incubated at room temperature with continuous stirring for 30 min, and activity was assayed every 5 min using the azocasein assay. The experiment was repeated with Cbfib2 (50 μL of 41 μM solution).

The effect of SBTI on enzyme activity was also investigated. Cbfib1.1 (50 μL of 9.2 μM solution) was added to 0.95 mL of 0.25 mg/mL SBTI in 0.1 M Tris buffer, pH 8.4, containing 0.05 M NaCl. The resulting solution was incubated at room temperature with continuous stirring for 30 min. Activity was assayed every 5 min with the azocasein assay. The experiment was repeated with Cbfib2 (50 μL of 8.2 μM solution).

Fibrinogen Degradation Studies. Fibrinogen (500 μL of 3.8 μM solution in 0.1 M phosphate buffer, pH 7.0, containing 0.15 M NaCl and 50 mM benzamidine) was pipetted into each of seven 1.5-mL microcentrifuge tubes. Cbfib1.1 (8.5 μL of 4.6 μM solution) was added to each tube to achieve a molar ratio of fibrinogen/enzyme of approximately 50. The resulting solution was incubated at 37 °C. At various times (0–120 min) the reaction in a selected tube was stopped by the addition of 250 μL of 250 mM EDTA solution followed by 500 μL of SDS–PAGE sample buffer. Aliquots were analyzed by SDS–polyacrylamide gel electrophoresis to determine the time sequence of fibrinogen chain cleavage. The experiment was repeated using Cbfib1.2 (6.6 μL of 5.8 μM enzyme solution) and 0.5 mL of 3.8 μM fibrinogen solution; Cbfib2 (11 μL of 3.5 μM solution); and Accfib (16 μL of 2.6 μM solution). In all cases the molar ratio of fibrinogen/enzyme was approximately 50. To determine the sequence of peptide bond cleavage events during the early stages of incubation, the experiments with Cbfib1.1 and Cbfib2 were repeated with time points ranging from 0 to 5 min.

Fibrin Degradation Studies. Fibrin was formed from plasminogen-free fibrinogen as follows: A total of 500 μL of 3.8 μM fibrinogen solution in 0.1 M Tris buffer and 0.05 M

NaCl, pH 8.3, was added to each of seven 1.5-mL microcentrifuge tubes. Topical thrombin (5 μL of 1000 units/mL) and 50 μL of 100 mM $CaCl_2$ were also added, and the resulting solution was incubated at 37 °C for 10 min. Following incubation, the resulting fibrin clot was washed three times by the addition of 0.75 mL of 0.1 M sodium phosphate buffer, pH 7.0, containing 0.15 M NaCl and 50 mM benzamidine. Subsequently, 0.5 mL of the same buffer was added followed by the addition of Cbfib1.1 (8.5 μL of 4.6 μM solution) to achieve a molar ratio of fibrin/enzyme of 50. The resulting solution was incubated at 37 °C. At various times (0–24 h) the reaction in a selected tube was stopped by the addition of 250 μL of 250 mM EDTA solution followed by 500 μL of SDS–PAGE sample buffer. Aliquots were analyzed by SDS–polyacrylamide gel electrophoresis to determine the time sequence of fibrin degradation. The experiment was repeated for Cbfib1.2 where 6.6 μL of 5.8 μM solution was added to each tube containing 0.5 mL of fibrin solution; Cbfib2 (11 μL of 3.5 μM solution); and Accfib (16 μL of 2.6 μM solution). In all cases the molar ratio of fibrin/enzyme was approximately 50.

Determination of Cleavage Sites. Fibrinogen (30 nmol) was dissolved in 2 mL of 0.1 M Tris buffer, pH 8.0, containing 50 mM benzamidine and 0.02% sodium azide. To this solution was added 13.5 μL of Cbfib1.1 (0.6 nmol). The solution was incubated at 37 °C for 1 min, and the reaction was stopped by the addition of 1 mL of 250 mM EDTA. The experiment was repeated with an incubation time of 5 min. The solutions were then brought to 8 M urea, and degraded fibrinogen was reduced and carboxymethylated. Reductive carboxymethylation was performed by the addition of dithiothreitol in a 10-fold molar excess over fibrinogen. After oxygen-free nitrogen was passed through the solution, it was incubated at room temperature for 1 h. Iodoacetamide was then added in a 10-fold molar excess over fibrinogen, and alkylation was allowed to proceed in the dark at room temperature for 1 h under oxygen-free nitrogen. For Cbfib2, the same fibrinogen solution was prepared, and 17.6 μL of Cbfib2 (0.6 nmol) was added to obtain a fibrinogen/Cbfib2 ratio of approximately 50. The solution was incubated at 37 °C for 2 min, and the reaction was stopped by the addition of 1 mL of 250 mM EDTA. The experiment was then repeated with an incubation time of 5 min as for Cbfib1.1. The solutions were brought to 8 M urea, and the proteolytically degraded fibrinogen was reduced and carboxymethylated as described above. Fibrinogen fragments were separated by reverse-phase HPLC on a Vydac C_4 column. The isolated peptides were further purified by reverse-phase chromatography on a Vydac C_{18} column, and the amino-terminal amino acid sequences (6–8 residues) were determined by automated gas-phase sequencing.

Results

Purification of Fibrinolytic Enzymes. Purification of the fibrinolytic enzyme from *C. basiliscus basiliscus* venom employed a three-step procedure including hydrophobic interaction HPLC, hydroxylapatite HPLC, and anion-exchange HPLC. Following hydrophobic interaction chromatography of crude venom, examination of the elution fractions using the fibrin-plate assay revealed two main activity peaks, named Cbfib1 and Cbfib2 (Figure 1). These two peaks were pooled separately and were further fractionated by hydroxylapatite chromatography. The fibrinolytic activity profile of Cbfib1 showed two main activity peaks, Cbfib1.1 and Cbfib1.2 (Figure 2A). The elution profile of Cbfib2 revealed a single activity peak (Figure 2B). Since SDS–PAGE and reverse-phase HPLC indicated that Cbfib.1 and Cbfib1.2 contained a number of contaminants after hydroxylapatite HPLC (Figure 3), they were further purified by anion-exchange chromatography (Figure 4). Both enzymes appear homogeneous by reverse-phase HPLC after anion-exchange chromatography (Figure 3); similarly, Cbfib2 appeared homogeneous after hydroxylapatite HPLC (Figure 3).

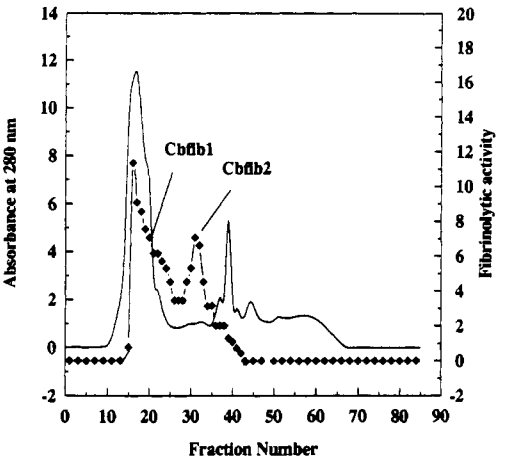

FIGURE 1: Hydrophobic interaction chromatography of *C. basiliscus basiliscus* venom. The solid line indicates effluent absorbance at 280 nm; (◆—◆) indicates fibrinolytic activity (expressed in cm^2 of fibrin plate cleared per 10 μL of fraction tested). Chromatography was performed as described under Materials and Methods.

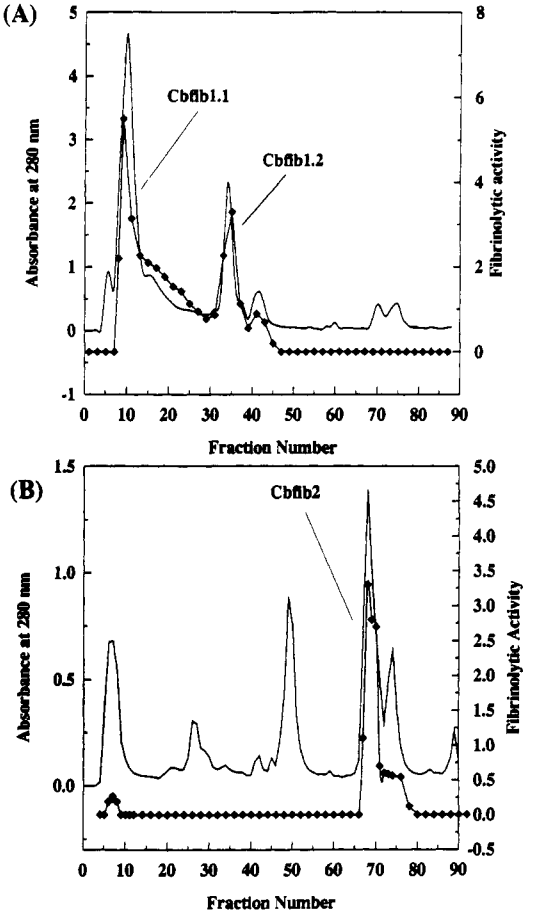

FIGURE 2: Hydroxylapatite chromatography of fibrinolytic activity pools resulting from hydrophobic interaction chromatography: (A) Cbfib1; (B) Cbfib2. The solid line indicates effluent absorbance at 280 nm; (◆—◆) indicates fibrinolytic activity as in Figure 1. Chromatography was performed as described under Materials and Methods.

Table I summarizes the purification procedure for the three enzymes. The recovery for each enzyme is quite low since they

Table I: Fibrinolytic Enzyme Purification

purification step	protein (mg)	activity (PIU)	specific activity (PIU/mg)	purification	recovery (% crude activity)
crude	579	89	0.15	0	100
after hydrophobic interaction chromatography					
Cbfib1[a]	241	74	0.31	2.1	83
Cbfib2	32	5.6	0.17	1.1	6.3
after hydroxylapatite chromatography					
Cbfib1.1	83	33.7	0.41	2.7	37.8
Cbfib1.2	42	18.5	0.44	2.9	20.1
Cbfib2[b]	7	3.5	0.50	3.3	3.9
after AX-300 chromatography					
Cbfib1.1	58	27.6	0.47	3.1	31
Cbfib1.2	34	17.1	0.50	3.3	19.2

[a] At this step Cbfib1.1 and Cibfib1.2 eluted together. [b] After this step Cbfib2 was homogeneous.

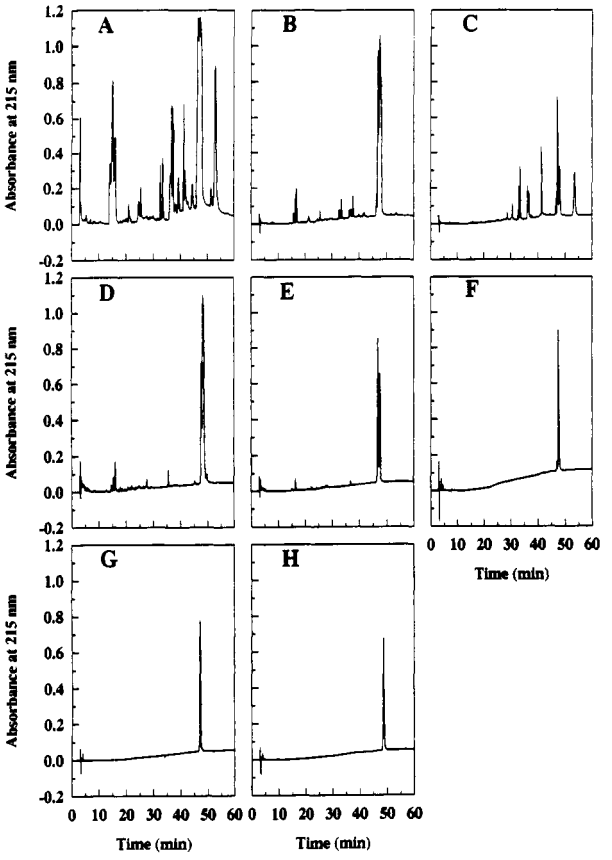

FIGURE 3: Determination of purity by reverse-phase chromatography. Aliquots from each purification step (50–100 μL) were injected into a Vydac C_4 column. The components were separated by the following elution protocol: 0–5-min isocratic elution with 90% solvent A (0.1% TFA in H_2O)–10% solvent B (0.1% TFA in 80% acetonitrile–20% H_2O); 55-min linear gradient to 80% solvent B. A flow rate of 1 mL/min was employed. The following elution profiles are shown: (A) crude venom; (B) Cbfib1 after hydrophobic interaction chromatography; (C) Cbfib2 after hydrophobic interaction chromatography; (D) Cbfib1.1 after hydroxylapatite chromatography; (E) Cbfib1.2 after hydroxylapatite chromatography; (F) Cbfib2 after hydroxylapatite chromatography; (G) Cbfib1.1 after anion-exchange chromatography; (H) Cbfib1.2 after anion-exchange chromatography.

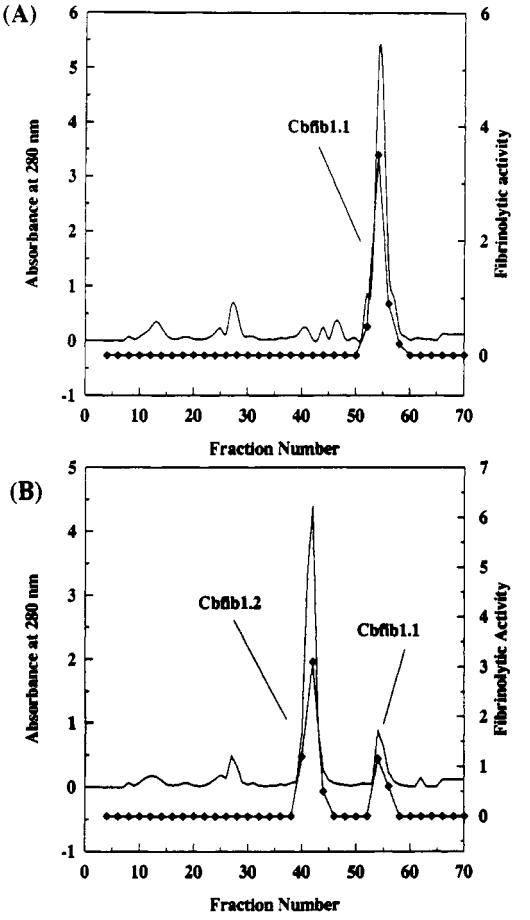

FIGURE 4: Anion-exchange chromatography for final purification of fibrinolytic components resulting from hydroxylapatite purification of Cbfib1: (A) Cbfib1.1; (B) Cbfib1.2. The solid line indicates effluent absorbance at 280 nm; (◆—◆) indicates fibrinolytic activity of resulting fractions (as in Figure 1). Chromatography was performed as described under Materials and Methods.

were purified separately. However, total recovery of activity for the three enzymes is over 50%. It should be noted that these three enzymes comprise a significant portion of the total venom protein, approximately 30%, with the major component being Cbfib1.1.

Physicochemical Properties. SDS–PAGE of the purified enzymes (Figure 5) reveals that the molecular weights of Cbfib1.1 and Cbfib1.2 are approximately 23 500. The molecular weight of Cbfib2 is slightly lower, approximately 22 500 (Figure 5). Isoelectric focusing revealed that both Cbfib1.1 and Cbfib1.2 have low isoelectric points at pH 4.1 and 4.7, respectively. By comparison Cbfib2 possessed a considerably higher isoelectric point at pH 8.5. The difference in isoelectric points between the enzymes suggests that the dissimilarities observed in molecular weights could be due to the influence of intrinsic charge differences on mobilities in SDS–PAGE. The amino acid compositions of the enzymes are presented in Table II. The number of residues has been estimated at approximately 211 in each enzyme. There is extensive similarity between Cbfib1.1 and Cbfib1.2 except for the number of valine residues. Cbfib2 appears similar to the other two enzymes except for an increased number of lysine and alanine residues. The fibrinolytic enzymes contain little or no carbohydrate as revealed by periodic acid–silver staining (Dubray

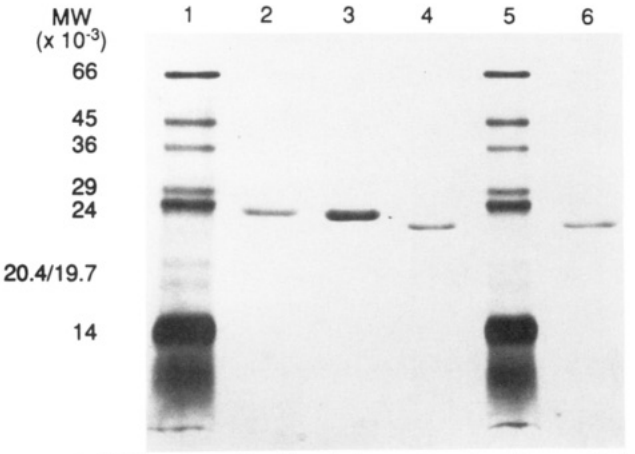

FIGURE 5: SDS–polyacrylamide gel electrophoresis of the purified fibrinolytic enzymes from *C. basiliscus basiliscus* venom. Lanes 1–6 contain the following: (1) SDS–PAGE standards; (2) Cbfib1.1, 0.8 μg; (3) Cbfib1.2, 1 μg; (4) Cbfib2, 0.9 μg; (5) SDS–PAGE standards; (6) Accfib, 0.9 μg. Proteins were visualized after Coomassie blue R250 staining followed by silver staining. Molecular weights of marker proteins are shown on the left.

Table II: Amino Acid Compositions of Fibrinolytic Enzymes[a]

amino acid	Cbfib1.1	Cbfib1.2	Cbfib2
Asp	27	26	25
Glu	22	20	21
Ser	21	20	18
Gly	14	12	15
His	9	9	8
Arg	15	15	14
Thr	12	11	11
Ala	11	9	15
Pro	8	7	8
Tyr	10	12	11
Val	13	19	13
Met	5	5	6
Ile	11	11	10
Leu	20	21	19
Phe	6	6	7
Lys	7	8	10
Cys	ND[b]	ND	ND
Trp	ND	ND	ND
sum	211	211	211

[a] Results are the average of two 24-h hydrolyses for each enzyme. [b] Not determined.

& Bezard, 1982). On the basis of the sensitivity of this procedure and the large amount of fibrinolytic enzymes applied to SDS–PAGE (30–50 μg), the content of carbohydrate, if present, must be less than 1%.

Inhibition Studies. Cbfib1.1 and Cbfib1.2 are fully inactivated within 5 min by incubation with a 5000-fold molar excess of EDTA. At a 200–1000-fold molar excess, activity loss varies from 20% to 75%. Cbfib1.1 and Cbfib1.2 do not lose activity upon incubation with serine protease inhibitors including SBTI (equal molar ratio) and PMSF (3.0 mM). Cbfib2 is fully inactivated within 5 min by incubation with a 1000-fold molar excess of EDTA, and although not affected by an equal molar ratio of SBTI, it is inhibited approximately 15% when treated with 3.0 mM PMSF. With Zincov, inhibition studies produced similar results for Cbfib1.1 and Cbfib1.2. When the enzymes were preincubated with the inhibitor and assayed in the presence of the inhibitor, 5% of azocaseinolytic activity remained at 16.5 mM Zincov concentration, 8% at 4.1 mM, and 12% at 1.0 mM. Without preincubation of the enzymes with Zincov, inhibition was considerably weaker: 80% of the original activity remained at 4.1 mM Zincov concentration. Similar weak competitive

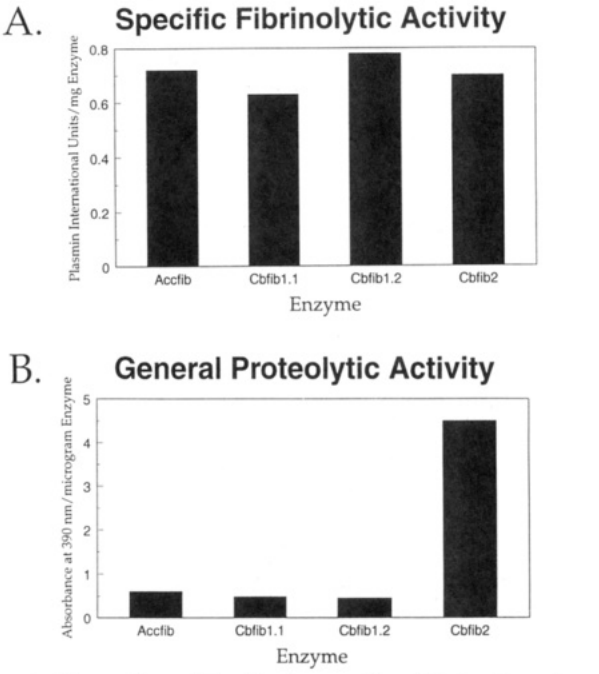

FIGURE 6: Comparison of functional properties of *C. basiliscus basiliscus* fibrinolytic enzymes: (A) specific fibrinolytic activity; (B) general proteolytic activity. Fibrinolytic and proteolytic activities were estimated as described under Materials and Methods.

inhibition by Zincov has been observed for Accfib (K_i = 16 mM), an enzyme whose zinc content has been directly measured by zinc metal analysis (Guan et al., 1991). Our findings suggest that the *C. basiliscus basiliscus* enzymes are also zinc-dependent and functionally similar to Accfib.

Proteolytic and Fibrinolytic Activities. Specific fibrinolytic activities for Cbfib1.1, Cbfib1.2, and Cbfib2 were measured and compared to that of Accfib (Figure 6A). The differences were minor with specific activities ranging around 0.7 PIU/mg of protein. However, general proteolytic activities (using azocasein as the substrate) showed wide divergence (Figure 6B). The specific azocaseinolytic activity of Cbfib2 is 7.9-fold higher than the corresponding activity of Accfib and 12-fold higher than Cbfib1.1 and Cbfib1.2. The specific azocaseinolytic activity of Cbfib1.1 and Cbfib1.2 is approximately 70% of that of Accfib. Using the skin hemorrhagic assay, modified from that previously described by Kondo et al. (1960), none of the fibrinolytic enzymes exhibited hemorrhagic activity as evidenced by a lack of extravascular bleeding on the underside of the mouse skin.

Tryptic Peptide Mapping. Comparison of tryptic digestion profiles of the *C. basiliscus basiliscum* fibrinolytic enzymes by C_{18} reverse-phase HPLC revealed, as other results already suggested, a significant degree of similarity between Cbfib1.1 and Cbfib1.2 (data not shown). However, differences in tryptic peptide elution patterns between these two enzymes are numerous enough not be be accounted for by a single amino acid substitution. In keeping with our other findings, Cbfib2 appears to be somewhat different from the other two enzymes basely solely on elution profiles from C_{18} reverse-phase HPLC. The three HPLC elution profiles revealed between 25 and 35 peptide peaks in each. This is fairly consistent with the lysine and arginine content of the enzymes, which varies between 22 and 24 residues. These results suggest that Cbfib1.1 and Cbfib1.2 are more closely related than Cbfib1.2 is to either of the other two. Nonetheless, all three have, most likely evolved from a common ancestral precursor.

Fibrin and Fibrinogen Degradation. All three *C. basiliscus*

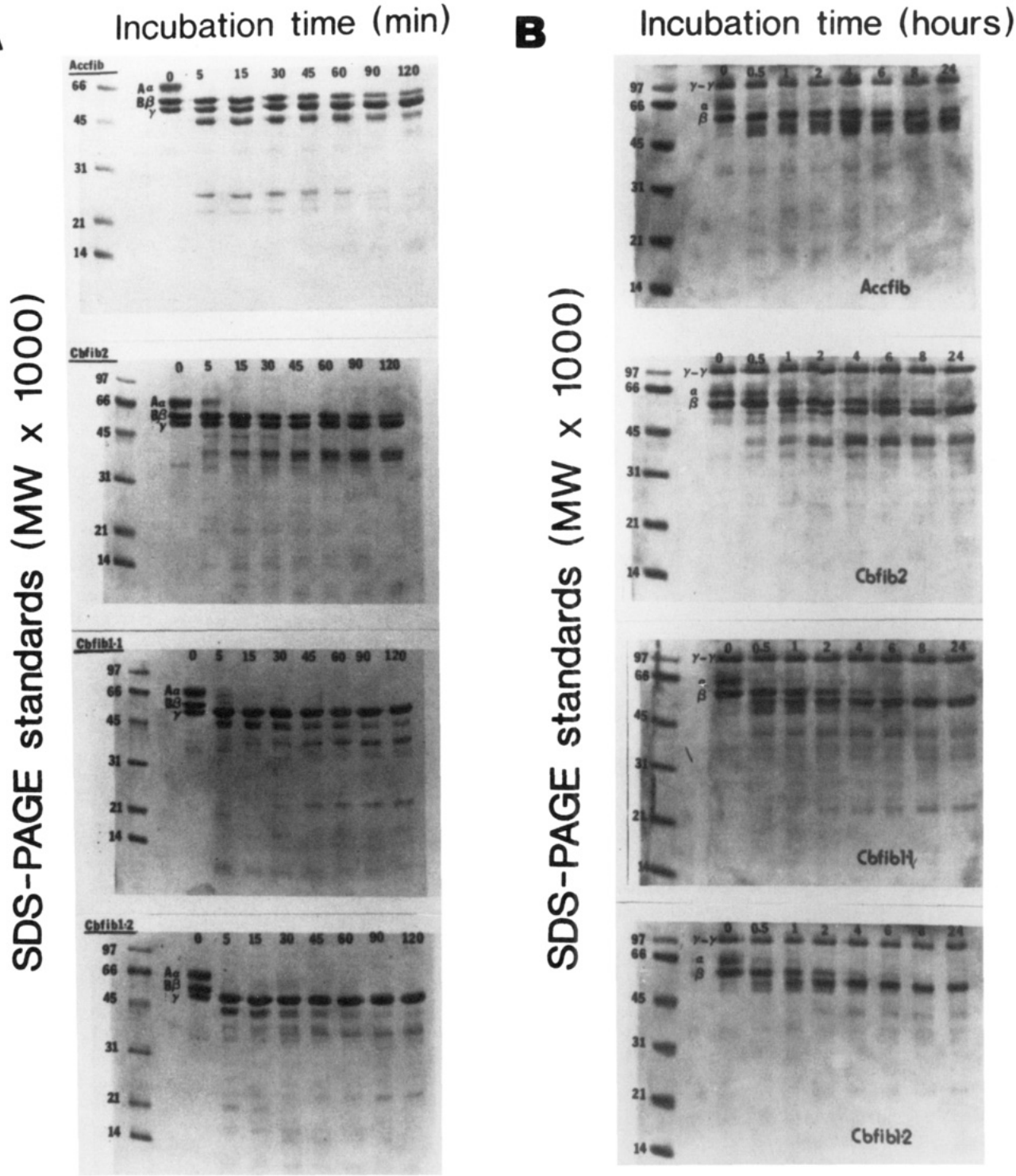

FIGURE 7: Effect of fibrinolytic enzymes on fibrinogen and fibrin: (A) time–course analysis by SDS–PAGE (10% acrylamide gels) of fibrinogen digestion; (B) time–course analysis by SDS–PAGE (10% acrylamide–8 M urea gels) of fibrin digestion. Digestions were performed as described under Materials and Methods. Staining was with Coomassie blue R250. Molecular weights of marker proteins are shown on the left.

enzymes degrade fibrin and fibrinogen, and they apparently degrade these proteins by cleavage of peptide bonds different from those cleaved by Accfib, a venom enzyme previously investigated for specific cleavage sites in fibrinogen (Retzios & Markland, 1988). The number of fibrin/fibrinogen cleavage products observed and the mode of action are identical for Cbfib1.1 and Cbfib1.2, indicating that these enzymes are functionally very similar, as well as being structurally related. However, Cbfib2 displays a fibrin/fibrinogen degradation profile that is substantially different from that of Cbfib1.1 and Cbfib1.2.

Figure 7 reveals the overall pattern of fibrinogen and fibrin degradation and indicates the differences between the cleavage patterns of the four fibrinolytic enzymes under study. It is immediately evident that whereas Accfib makes a single initial cleavage on the Aα-chain and degrades the Bβ-chain much more slowly, Cbfib1.1 and Cbfib1.2 catalyze a number of cleavages and degrade the Bβ-chain much faster than Accfib. In contrast, Cbfib2 degrades the Bβ-chain even more slowly than Accfib, and it cleaves the Aα-chain at several positions which are different from those cleaved by Cbfib1.1, Cbfib1.2, and Accfib. None of these enzymes appear to degrade the

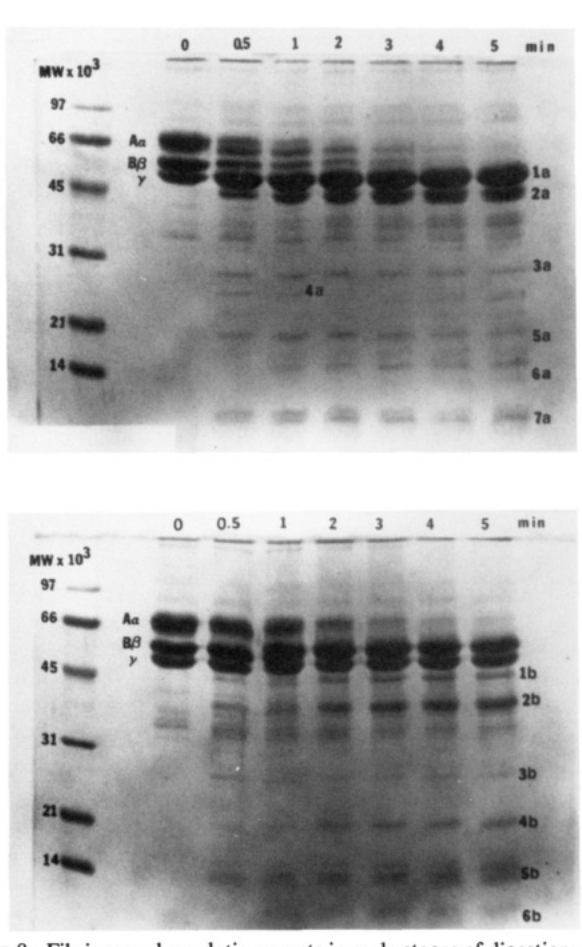

FIGURE 8: Fibrinogen degradation events in early stages of digestion: time–course analysis by SDS–PAGE (10% acrylamide gels) of fibrinogen digestion by (A) Cbfib1.1 and (B) Cbfib2. Staining was with Coomassie blue R250. Molecular weights of marker proteins are shown on the left.

γ-chain. This is substantiated in addition to the findings in Figure 7 by those described following short-term incubation with fibrinogen (described below and see Figure 8). Although the Bβ-chain main cleavage fragment overlaps the γ-chain band in Figure 7A in all the enzymes examined, the intensity of the bands does not change over time, indicating that both the Bβ-chain main fragment and the γ-chain do not undergo lysis. Additionally, Figure 7B shows that the γ–γ dimer is not affected by any of the fibrinolytic enzymes. When the degradation of fibrin by the four enzymes (Figure 7B) is compared, degradation profiles for all enzymes were similar to the pattern displayed for fibrinogen although digestion times are longer with fibrin.

Figure 8 shows the events in the early phases of fibrinogen degradation by Cbfib1.1 and Cbfib2 (1–5 min). It is apparent that, at the ratio of substrate to enzyme selected (50/1), there is no difference in the rate of Aα-chain and Bβ-chain digestion for Cbfib1.1. The major product of the digestion for Cbfib1.1 (Figure 8A) is a polypeptide of molecular weight 45 000 (product 2a). It is also evident (Figure 8B) that the same product is present in very low amounts in Cbfib2 (product 1b). Cbfib2 also produces a group of breakdown products at a molecular weight of approximately 38 000 (product 2b) which are present in substantially lower amounts in the Cbfib1.1 fibrinogen digest. Fibrinopeptides at molecular weights of approximately 25 000, 20 000, and 15 000 are produced by both enzymes, but the 25 000 fragment (product 4a) is very short-lived in the Cbfib1.1 digest. The 20 000 fragment

Table III: N-Terminal Amino Acid Sequence of Fibrinogen Degradation Products following Digestion with Cbfib1.1 or Cbfib2

peptide no.	amino-terminal sequence of fibrinogen fragment[a]
Cbfib1.1 digestion	
1	Leu-Val-Thr-Ser-Lys-Gly-Asp-?-Lys-
2	Thr-Gly-Lys-Asn-?-?-Gly-Phe-Phe-Ser-
3	Ser-Lys-Gln-Phe-Thr-Ser-?-?-?-Tyr-
4	?-Gly-Val-Asn-Asp-Asn-Glu
Cbfib2 digestion	
1	Met-Leu-Gly-Glu-Phe-Val-Ser-Glu-?-Glu-?-?-Gly-Ser-
2	Ser-Thr-Ser-?-Gly-Thr-Gly-?-?-?-Glu-
3	Ser-Thr-Ser-?-Gly-?-Gly-Gly-?-Glu

[a] Fragments were isolated and purified as outlined under Materials and Methods. A ? indicates that the amino acid was not identified in the sequence.

(product 4b) appears to accumulate after Cbfib2 digestion, but it is further degraded by Cbfib1.1 (product 5a). An extra fragment of molecular weight 28 000 is produced in the Cbfib1.1 digest (product 3a) which has no detectable equivalent in the Cbfib2 digest. A number of peptides of approximately 12 kDa are evident in the Cbfib2 fibrinogen digestion (product 5b); these are substituted by lower molecular weight products in the Cbfib1.1 digest (product 7a).

From the increased intensity with time of the band in the γ-chain region at 50 kDa in the Cbfib1.1 digest (Figure 8A), it would appear that a Bβ-chain degradation product comigrates with the γ-chain on SDS–PAGE (product 1a). Since there is no evident decrease in intensity of this component during the time course of this experiment, it would appear that this fragment is not further degraded. This 50-kDa peptide was assumed to be a Bβ-derived product since comparison with Accfib indicates that the major product at 45 kDa (product 2a) is derived from the Aα-chain. Further, Cbfib2, which degrades the Bβ-chain very slowly, does not contain a digestion product which comigrates with the γ-chain (Figure 8B).

Determination of Cleavage Sites. In order to determine the sites of the initial cleavages in fibrinogen, we incubated larger amounts of fibrinogen (30 nmol) with Cbfib1.1 and Cbfib2 at a molar ratio of 50/1 (a ratio kept constant throughout these experiments) for 1 and 2 min, respectively, and for 5 min each, and isolated the resultant cleavage products. The short incubation times were employed on the basis of the results of the previous experiment (shown in Figure 8) as being optimal for the accumulation of early degradation products.

Following digestion the reactions were stopped by the addition of EDTA, and samples were reduced and carboxymethylated (see Materials and Methods). The digests were analyzed by reverse-phase chromatography. Peptides were purified by C_4 and C_{18} reverse-phase chromatography, and their amino-terminal sequences were determined (Table III). To establish the sites of cleavage, amino-terminal sequences of the fibrinogen degradation peptides were compared and fitted to the known sequence of the Aα-chain of human fibrinogen (Henschen et al., 1983).

Sequence analysis of the products of digestion suggests that Cbfib1.1 cleaves the Aα-chain at Lys^{413}–Leu^{414} (peptide 1 in Table III), Ser^{505}–Thr^{506} (peptide 2), and Tyr^{560}–Ser^{561} (peptide 3). The Lys^{413}–Leu^{414} cleavage site has also been identified as the primary Accfib cleavage site in the Aα-chain of fibrinogen (Retzios & Markland, 1988). The two other cleavage sites are quite unusual for a zinc-dependent enzyme. The sequence of fragment 4 corresponds to the sequence of the amino terminus of the Bβ-chain of fibrinogen. The molecular weight of this fragment, as determined by SDS–PAGE,

Table IV: Primary Structure of the Aα-Chain of Fibrinogen Cleavage Sites for Cbfib1.1 and Cbfib2 Covering the P_7 to the P_7' Subsites[a]

	P_7	P_6	P_5	P_4	P_3	P_2	P_1	P_1'	P_2'	P_3'	P_4'	P_5'	P_6'	P_7'
Cbfib1.1 cleavage sites in the Aα-chain of fibrinogen														
site 1 (residues 407–420)	R	E	Y	H	T	E	K	L	V	T	S	K	G	D
site 2 (residues 499–512)	A	F	F	D	T	A	S	T	G	K	T	F	P	G
site 3 (residues 554–567)	R	G	K	S	S	S	Y	S	K	Q	F	T	S	S
Cbfib2 cleavage sites in the Aα-chain of fibrinogen														
site 1 (residues 510–523)	F	P	G	F	F	S	P	M	L	G	E	F	V	S
site 2 (residues 248–261)	N	E	I	T	R	G	G	S	T	S	Y	G	T	G

[a] The position of the amino acid was assigned using the terminology of Schechter and Berger (1967).

is approximately 9000–10 000. It is obvious, therefore, that the cleavage site in the Bβ-chain is close to the amino terminus.

Sequence analysis of the cleavage products derived following Cbfib2 incubation with fibrinogen reveals that the major cleavage sites are located in the Aα-chain at Pro^{516}–Met^{517} (peptide 1 in Table III), and Gly^{254}–Ser^{255} (peptide 2). Peptides 2 and 3 (Table III) have the same amino-terminal sequence but molecular weights of 10 000 and 40 000, respectively. The small size of peptide 2 suggests the possibility that Cbfib2 catalyzes another cleavage in the Aα-chain between residues 330 and 360, although this fragment has not yet been identified. On the basis of our previous findings with Accfib digestion of fibrinogen (Retzios & Markland, 1988), the 45-kDa fibrinogen fragment (although not sequenced) results from digestion of the Aα-chain by Cbfib2 at Lys^{413}–Leu^{414}. This fragment is produced in small amounts following Cbfib2 digestion (Figure 8B, product 1b), suggesting that cleavage occurs slowly at the Lys^{413}–Leu^{414} position. Cleavage sites in the Aα-chain of fibrinogen are summarized in Table IV.

Discussion

Our findings indicate that Cbfib1.1 and Cbfib1.2 are not only structurally related but also cleave similar peptide bonds in fibrin and fibrinogen. The main difference from other fibrinolytic metalloproteases studied to date, including atroxase from *C. atrox* (western diamondback rattlesnake; Willis & Tu, 1988) and fibrolase (Accfib) from *A. contortrix contortrix* (southern copperhead; Retzios & Markland, 1988) venoms, is that the *C. basiliscus basiliscus* enzymes cleave the Bβ-chain of fibrinogen almost as readily as the Aα-chain. In fact, at molar ratios of 1/50 (enzyme/substrate) there is no apparent difference in degradation rates between the Aα- and Bβ-chains. Interestingly, atroxase and fibrolase cleave the Aα-chain preferentially; the Bβ-chain is degraded subsequently. By contrast, following 1-h incubation, the fibrinolytic enzyme from *Agkistrodon contortrix mokasen* (northern copperhead) venom degrades only the Aα-chain (Moran & Geren, 1981). The venom fibrinolytic enzymes studied thus far exhibit virtually no hydrolytic activity on the γ-chain of fibrinogen.

Immunological (western) blotting showed that the antibody to Accfib reacted very weakly, if at all, with purified Cbfib1.1 and Cbfib2 (Chen et al., 1991). This suggests that the enzymes, although being somewhat structurally related and most likely belonging to the same family of low molecular weight snake venom metalloproteinases, may be immunologically distinct. This may be of interest for potential clinical application of these enzymes (see below).

With fibrin as substrate, Cbfib1.1 and Cbfib1.2 exhibit a considerably slower degradation of the β-chain compared to the α-chain, probably due to steric hindrance induced by γ-chain cross-linking. Nonetheless, the rate of β-chain digestion is more rapid than that produced by Accfib under identical incubation conditions (1/50 molar ratio of venom fibrinolytic enzyme to substrate). Cbfib1.1 and Cbfib1.2 also show a broader specificity of cleavage sites than Accfib, although Lys^{413}–Leu^{414}, the primary cleavage site of Accfib in the α-chain of fibrinogen and fibrin (Retzios & Markland, 1988), is among these sites. In view of the broader specificity on fibrinogen displayed by the *C. basiliscus basiliscus* enzymes, it is surprising that these enzymes possess lower general proteolytic (azocaseinolytic) activity than Accfib (Figure 6). Lower activity toward the general protease substrate azocasein may signify a higher degree of specialization toward fibrin/fibrinogen than Accfib. The general similarity in fibrinolytic activities between all the venom enzymes tested (Figure 6A) might reveal deficiencies in sensitivity of the in vitro assay used (Bajwa et al., 1980) to determine fibrinolytic potential. A dynamic in vitro assay, assessing structural integrity of a fibrin clot, or in vivo clot dissolution studies would make such comparisons more valid.

Cbfib2 varies significantly both structurally and functionally from Cbfib1.1 and Cbfib1.2, although, like the other enzymes, it is also a metalloproteinase. Fibrinolytic activity of Cbfib2 is confined mainly to the α-chain of fibrin and fibrinogen, like Accfib. However, unlike Accfib, it shows only limited cleavage of the Lys^{413}–Leu^{414} bond, indicating structural differences in the active site geometry. Surprisingly, Cbfib2 possesses significantly higher levels of general proteolytic (azocaseinolytic) activity, approximately 8–12-fold higher, than the other enzymes studied (Figure 6B). This increased proteolytic activity is not evidenced by increased hemorrhagic activity since Cbfib2, as well as Cbfib1.1 and Cbfib1.2, showed no such activity following subcutaneous injection of large amounts of the enzymes (50–100 μg) into the backs of anesthetized mice. Hemorrhagic activity is defined as the ability to cause local hemorrhaging following intradermal injection of venom fractions into backs of depilated laboratory animals (Kondo et al., 1960).

Recently, two hemorrhagic proteinases, B1 and B2, were purified and characterized from *C. basiliscus basiliscus* venom (Molina et al., 1990). These enzymes are very similar to the fibrinolytic proteinases we describe; B1 has a molecular weight of 27 000 and p*I* of 9.8, and B2 has a molecualr weight of 27 500 and p*I* of 5.3. Both proteins are inhibited by EDTA, both degrade fibrin and fibrinogen, but they do not cross-react antigenically. Although appearing to be very similar to the fibrinolytic enzymes, they must be different since the fibrinolytic enzymes that we have purified possess virtually no hemorrhagic activity. Whether the hemorrhagic proteinases were contaminated by very similar fibrinolytic enzymes remains to be determined.

Amino acid analysis suggests that the Cbfib enzymes contain approximately 210 amino acid residues. Hemorrhagic and fibrinolytic venom metalloproteinases of known sequence contain 201–203 amino acids (Miyata et al., 1989; Shannon et al., 1989; Takeya et al., 1989). Accfib contains 203 amino acids (Guan et al., 1991; Randolph et al., 1992) and displays a significant degree of identity with the hemorrhagic metalloproteinases. All of these enzymes contain the sequence

His-Glu-Xaa-Gly-His-Asn-Leu-Gly (where Xaa is the hydrophobic residue leucine, isoleucine, or methionine). This signature sequence contains the putative zinc-chelating residues (two histidine residues separated by three amino acids) and the catalytic glutamic acid residue (Takeya et al., 1990) identified by homology with the zinc-chelating sequence of thermolysin (Colman et al., 1972). However, the difference in kinetics of inhibition of the venom metalloproteinases by Zincov as compared to thermolysin (a zinc-dependent, bacterial fibrinolytic metalloproteinase) is considerable (K_i for thermolysin is 0.48 μM; Nishiro & Powers, 1979), suggesting that the zinc atom may be oriented differently in the active site of the venom fibrinolytic enzymes. It would appear, therefore, that there is a family of evolutionarily related venom metalloproteinases distributed widely throughout different genera of the *Crotalidae* family, including *Agkistrodon*, *Trimeresurus*, and *Crotalus* and, perhaps, even more widely in other snake families. These small metalloproteinases possess strikingly similar sequences and physicochemical properties but have different biological activities.

Analysis of the primary structure around the peptide bonds cleaved in fibrinogen by the fibrinolytic enzymes from *C. basiliscus basiliscus* venom from the P_7 to the P_7' subsites (Table IV) fails to show a requirement for any preferred amino acid residues that determine cleavage specificity. The only possible pattern emerging is the presence of threonine or serine (hydroxyl amino acids) in the P_3 subsite for Cbfib1.1. These findings suggest that bond cleavage specificity must be guided at least in part by secondary and tertiary structure determinants in fibrinogen. The fibrinolytic enzymes from *C. basiliscus basiliscus* venom appear to exhibit quite unusual bond cleavage specificity with the natural substrates, fibrin or fibrinogen. Cbfib1.1 cleaves at the same Lys^{413}–Leu^{414} bond in the Aα-chain of fibrinogen as fibrolase, the fibrinolytic enzyme from southern copperhead venom (Retzios & Markland, 1988). However, additional cleavages occur at Ser^{505}–Thr^{506} and Tyr^{560}–Ser^{561} in the Aα-chain. Cleavage sites catalyzed by Cbfib2 are also unusual: Pro^{516}–Met^{517} and Gly^{254}–Ser^{255} in the Aα-chain of fibrinogen.

The study of fibrinolytic enzymes from various sources, such as Cbfib1.1, Cbfib1.2, and Cbfib2, may have direct applications. Accfib, the properties of which were compared to those of the C. *basiliscus basiliscus* enzymes in this study, was shown to be as effective as streptokinase in dissolving clots in animal models (Markland et al., 1989) without unexpected complications. Accfib, which has higher general proteolytic activity than Cbfib1.1, was also shown to have a very limited, if any, effect on several components of the fibrinolytic system (Retzios & Markland, 1988). Other venom fibrinolytic enzymes showed similar promise (Willis & Tu, 1989). The advantage of such enzymes is that their action is not dependent on plasminogen activation, and their disadvantages are no worse than those of streptokinase, the use of which is gaining momentum in thrombolytic therapy. Additionally, the venom-derived enzymes may act synergistically with plasminogen activators, thereby providing an intriguing potential clinical application for these enzymes. Further structural studies of these enzymes will elucidate their mode of action, and information derived may be used in thrombolytic agent design.

ACKNOWLEDGMENTS

We extend our appreciation to Dr. John Tomich, Director, Medical Genetics Microchemical Facility, Children's Hospital of Los Angeles, for sequence determination and to the UCLA Protein Microsequencing Laboratory for amino acid analyses. The skillful technical assistance provided by Rita Oregon is also gratefully acknowledged.

Registry No. Fibrinogenase, 9002-04-4; metalloproteinase, 81669-70-7; fibrinase, 9001-90-5.

REFERENCES

Bajwa, S. S., Markland, F. S., & Russel, F. E. (1980) *Toxicon 18*, 285–290.

Bidlingmeyer, B. A., Cohen, S. A., & Tarvin, T. L. (1984) *J. Chromatogr. 336*, 93–104.

Charney, J., & Tomarelli, R. M. (1947) *J. Biol. Chem. 171*, 501–505.

Chen, H. M., Guan, A. L., & Markland, F. S. (1991) *Toxicon 29*, 683–694.

Colman, P. M., Jansonius, J. N., & Matthews, B. W. (1972) *J. Mol. Biol. 70*, 701–724.

Didisheim, P., & Lewis, J. H. (1956) *Proc. Soc. Exp. Biol. Med. 93*, 10–13.

Dubray, G., & Bezard, G. (1982) *Anal. Biochem. 119*, 325–329.

Guan, A. L., Retzios, A. D., Henderson, G. N., & Markland, F. S. (1991) *Arch. Biochem. Biophys. 289*, 197–207.

Henschen, A., Lottspeich, F., Kehl, M., & Southan, C. (1983) *Ann. N.Y. Acad. Sci. 408*, 28–43.

Holeman, W. H., & Weiss, L. J. (1976) *J. Biol. Chem. 251*, 1663–1669.

Kondo, H., Kondo, S., Ikezawa, H., Murata, R., & Ohsaka, A. (1960) *Jpn. J. Med. Sci. Biol. 13*, 43–51.

Kornalik, F. (1966) *Mem. Inst. Butantan Symp. Int. 33*, 179–188.

Laemmli, U. K. (1970) *Nature 227*, 680–685.

Markland, F. S., & Damus, P. W. (1971) *J. Biol. Chem. 246*, 6460–6473.

Markland, F. S., Reddy, K. N. N., & Guan, A. L. (1988) in *Hemostasis and Animal Venoms* (Pirkle, H., & Markland, F. S., Eds.) pp 173–189, Marcel Dekker, Inc., New York.

Markland, F. S., Bookstein, J. J., & Machado, T. (1989) *Thromb. Haemostasis 62*, 121.

Merrill, C. R., Goldman, D., Sedman, S. A., & Ebert, M. H. (1983) *Science 121*, 1437–1438.

Miyata, T., Takeya, H., Ozeki, Y., Arakaw, M., Tokunaga, F., Iwanaga, S., & Omori-Satoh, T. (1989) *J. Biochem. 105*, 847–853.

Molina, O., Seriel, R. K., Martinez, M., Sierra, M. L., Varela-Ramirez, A., & Rael, E. D. (1990) *Int. J. Biochem. 22*, 253–261.

Moran, J. B., & Geren, C. R. (1981) *Biochim. Biophys. Acta 659*, 161–168.

Nishiro, N., & Powers, J. C. (1979) *Biochemistry 18*, 4340–4347.

Ouyang, C., & Teng, C.-M. (1972) *Biochim. Biophys. Acta 278*, 155–162.

Randolph, A., Chamberlain, S. H., Chu, H.-L., Retzios, A. D., Markland, F. S., & Masiarz, F. R. (1992) *Protein Sci.* (in press).

Retzios, A. D., & Markland, F. S. (1988) *Thromb. Res. 52*, 541–552.

Retzios, A. D., & Markland, F. S. (1990) *Protein Expression Purif. 1*, 33–39.

Schechter, I., & Berger, A. (1967) *Biochem. Biophys. Res. Commun. 27*, 157–162.

Shannon, J. D., Baramova, E. N., Bjarnason, J. B., & Fox, J. W. (1989) *J. Biol. Chem. 264*, 11575–11583.

Takeya, H., Arakawa, M., Miyata, T., Iwanaga, S., & Omori-Satoh, T. (1989) *J. Biochem. 106*, 151–157.

Takeya, H., Oda, K., Miyata, T., Omori-Satoh, T., & Iwanaga, S. (1990) *J. Biol. Chem. 265*, 16068–16073.
Teng, C.-M., & Seegers, W. H. (1981) *Thromb. Res. 23*, 255–263.
Willis, T. W., & Tu, A. T. (1988) *Biochemistry 27*, 4769–4777.
Willis, T. W., Tu, A. T., & Miller, C. W. (1989) *Thromb. Res. 53*, 19–29.

Interaction of the N-Terminal Region of Hirudin with the Active-Site Cleft of Thrombin

Andreas Betz, Jan Hofsteenge, and Stuart R. Stone*,‡
Friedrich Miescher-Institut, P.O. Box 2543, CH-4002 Basel, Switzerland
Received October 21, 1991; Revised Manuscript Received January 31, 1992

ABSTRACT: Site-specific substitutions of the first five amino acids of the thrombin inhibitor hirudin have been made and the effects of these substitutions on the kinetics of formation of the thrombin–hirudin complex evaluated. The effects of different substitutions of Val1 indicate that nonpolar interactions play a major role in the binding of this residue. In the second position (Val2), polar amino acids were better accommodated than in the first. The mutant with arginine in the second position bound particularly well to thrombin; its dissociation constant was 9-fold lower than that of wild-type recombinant hirudin. Comparison of the effects of single and double mutations involving Val1 and Val2 indicates that there was no cooperativity in the binding of these two residues. Elimination of the hydrophobic interactions made by the aromatic ring of Tyr3 of hirudin resulted in a large loss of binding energy (12.7 kJ mol^{-1}). Replacement of Thr4 of hirudin by serine and alanine suggested that both the γ-methyl and the hydroxyl group of the threonine were important in the stabilization of the thrombin–hirudin complex. Replacement of Asp5 of hirudin by alanine and glutamate caused about the same loss in binding energy (5 kJ mol^{-1}). The effects of site-specific substitutions are discussed in terms of the crystal structure of the thrombin–hirudin complex. Molecular modeling provided plausible explanations for many of the observed effects. For instance, such studies suggested that the improved binding of the mutant with arginine in the second position could be due to an interaction of the arginine with the primary specificity pocket.

The crystal structures of thrombin–hirudin complexes indicate that hirudin inhibits thrombin by a previously unobserved mechanism for proteinase inhibition (Rydel et al., 1990, 1991; Grütter et al., 1990). The three N-terminal amino acids of hirudin are bound in the active-site cleft of thrombin while the C-terminal region of hirudin is bound to a positively charged surface groove on thrombin. The first three residues of hirudin form a parallel β-sheet with residues Ser214–Gly219[1] of thrombin. The orientation of the hirudin polypeptide chain within the active site is opposite of that observed with other inhibitors which form an antiparallel β-sheet with residues Ser214–Gly219. The α-amino group of hirudin forms hydrogen bonds with the carbonyl of Ser214 and the hydroxyl of Ser195 (Rydel et al., 1990, 1991). As shown in Figure 1, the side chain of the first amino acid [Val1′ in recombinant hirudin variant 1 (rhir)[2] and Ile1′ in recombinant hirudin variant 2, Lys47] makes numerous nonpolar interactions with thrombin residues including His57, Tyr60A, Trp60D, and Leu99 (Rydel et al., 1990, 1991; Grütter et al., 1990). The second residue of hirudin is located at the edge of the primary specificity pocket but, unlike other inhibitors of serine proteinases, does not penetrate this pocket. Tyr3′ is buried in a hydrophobic pocket constituted by residues Tyr60A, Ile174, Trp60D, and Leu99 of thrombin (Figure 1). This binding site is occupied by the D-phenylalanine of the inhibitor D-Phe-Pro-ArgCHCl$_2$ and has been called the aryl-binding pocket (Bode et al., 1989, 1990). The active site of thrombin is closed off by the N-terminal core domain of hirudin, and Thr4′ and Asp5′ seem to be important for the positioning of the core domain. A hydrogen bond between O^{γ} of Thr4′ and the ϵ-amino group of Lys47′ is thought to stabilize and position the core domain (Rydel et al., 1990, 1991). The orientation of the core domain is also aided by a salt bridge made between Asp5′ and Arg221A of thrombin (Figure 1; Rydel et al., 1990, 1991). This salt bridge should also make a direct contribution to the binding energy.

Previous investigations established a role for hydrophobic interaction with the three N-terminal amino acids of hirudin in the formation of the thrombin–hirudin complex (Wallace et al., 1989; Winant et al., 1991; Lazar et al., 1991). In the present study, site-directed mutagenesis has been used to study cooperative effects in the binding of the first two amino acids. In addition, the importance of the interactions made by Tyr3′, Thr4′, and Asp5′ has been examined. The changes in the binding energies (ΔG°_{b}) for the mutant hirudins were interpreted in terms of the crystal structures of the complexes and allowed the quantitative assessment of the importance of contacts revealed by these structures.

* Address correspondence to this author.
‡ Present address: Department of Haematology, University of Cambridge, MRC Centre, Hills Road, Cambridge CB2 2QH, United Kingdom.

[1] The numbering of the thrombin is that of Bode et al. (1989) and is based on chymotrypsin numbering. Residues in recombinant hirudin are distinguished from those in thrombin by the use of primed numbers.
[2] Abbreviation: rhir, recombinant hirudin variant 1.

0006-2960/92/0431-4557$03.00/0